Mannose supplements induce embryonic lethality and blindness in phosphomannose isomerase hypomorphic mice

Vandana Sharma,* Jonamani Nayak,* Charles DeRossi,*,[1] Adriana Charbono,* Mie Ichikawa,* Bobby G. Ng,* Erika Grajales-Esquivel,† Anand Srivastava,*,[1] Ling Wang,* Ping He,* David A. Scott,* Joseph Russell,*,[1] Emily Contreras,*,[1] Cherise M. Guess,*,[1] Stan Krajewski,* Katia Del Rio-Tsonis,† and Hudson H. Freeze*,[2]

*Sanford-Burnham Medical Research Institute (SBMRI), La Jolla, California, USA; and †Department of Biology, Miami University, Oxford, Ohio, USA

ABSTRACT **Patients with congenital disorder of glycosylation (CDG), type Ib (MPI-CDG or CDG-Ib) have mutations in phosphomannose isomerase (*MPI*) that impair glycosylation and lead to stunted growth, liver dysfunction, coagulopathy, hypoglycemia, and intestinal abnormalities. Mannose supplements correct hypoglycosylation and most symptoms by providing mannose-6-P (Man-6-P) *via* hexokinase. We generated viable *Mpi* hypomorphic mice with residual enzymatic activity comparable to that of patients, but surprisingly, these mice appeared completely normal except for modest (~15%) embryonic lethality. To overcome this lethality, pregnant dams were provided 1–2% mannose in their drinking water. However, mannose further reduced litter size and survival to weaning by 40 and 66%, respectively. Moreover, ~50% of survivors developed eye defects beginning around midgestation. Mannose started at birth also led to eye defects but had no effect when started after eye development was complete. Man-6-P and related metabolites accumulated in the affected adult eye and in developing embryos and placentas. Our results demonstrate that disturbing mannose metabolic flux in mice, especially during embryonic development, induces a highly specific, unanticipated pathological state. It is unknown whether mannose is harmful to human fetuses during gestation; however, mothers who are at risk for having MPI-CDG children and who consume mannose during pregnancy hoping to benefit an affected fetus *in utero* should be cautious.—Sharma, V., Nayak, J., DeRossi, C., Charbono, A., Ichikawa, M., Ng, B. G., Grajales-Esquivel, E., Srivastava, A., Wang, L., He, P., Scott, D. A., Russell, J., Contreras, E., Guess, C. M., Krajewski, S., Del Rio-Tsonis, K., Freeze, H. H. Mannose supplements induce embryonic lethality and blindness in phosphomannose isomerase hypomorphic mice. *FASEB J.* 28, 1854–1869 (2014). www.fasebj.org**

Key Words: congenital disorder of glycosylation · MPI-CDG · lens · eye defects

A POTENTIALLY LETHAL form of rare congenital disorder of glycosylation (CDG), type Ib [CDG-Ib; or phosphomannose isomerase (MPI)-CDG] can be treated with mannose as a dietary supplement (1). Supplementation overcomes impaired glycosylation caused by hypomorphic mutations in *MPI* because mannose bypasses the impaired conversion of fructose-6-phosphate (Fru-6-P) to mannose-6-phosphate (Man-6-P), which is the major source of Man-6-P derived from glucose. Mannose alleviates patients' stunted growth, hypoglycemia, liver dysfunction, coagulopathy, and protein-los-

Abbreviations: AAT, α-1 antitrypsin; AGA, aspartyl glucosaminidase; β-hex, β-hexosaminidase; BSA, bovine serum albumin; BSTFA, *N,O-bis*-[trimethylsilyl]trifluoroacetamide; CDG, congenital disorder of glycosylation; DMEM, Dulbecco's modified Eagle's medium; ECM, extracellular matrix; FACE, fluorophore-assisted carbohydrate electrophoresis; Fru-6-P, fructose-6-phosphate; G6PD, glucose-6-phosphate dehydrogenase; GC-MS, gas chromatography-mass spectrometry; Glc-6-P, glucose-6-phosphate; H&E, hematoxylin and eosin; HK, hexokinase; Man-6-P, mannose-6-phosphate; KI, knock-in; KO, knockout; mEF, mouse embryonic fibroblast; MPI, phosphomannose isomerase; PBS, phosphate-buffered saline; PGI, phosphoglucose isomerase; PLE, protein-losing enteropathy; PMM2, phosphomannomutase; RPE, retinal-pigmented epithelium; TCA, trichloroacetic acid; TNF-α, tumor necrosis factor α; WT, wild type

[1] Current address: C.D., Center for Child and Adolescent Medicine and Center for Metabolic Diseases Heidelberg, Department Kinderheilkunde I, Heidelberg, Germany; A.S., Global Institute of Stem Cell Therapy and Research, 4370 La Jolla Village Dr., San Diego, CA 92122, USA; J.R., Janssen Research and Development, LLC, 3210 Merryfield Row, San Diego, CA 92121, USA; E.C., Riley Children's Specialists, 11725 N. Illinois St., Ste. 240, Carmel, IN 46032, USA; C.M.G., St. Jude Children's Research Hospital, 262 Danny Thomas Pl., Memphis, TN 38105-2794, USA.

[2] Correspondence: Sanford-Burnham Medical Research Institute (SBMRI), 10901 North Torrey Pines Road, La Jolla, CA 92037, USA. E-mail: hudson@sanfordburnham.org

doi: 10.1096/fj.13-245514

This article includes supplemental data. Please visit *http://www.fasebj.org* to obtain this information.

0892-6638/14/0028-1854 © FASEB

ing enteropathy (2). Exogenous mannose is converted to Man-6-P by hexokinase (HK), replenishing this deficient precursor needed for multiple glycosylation pathways, including the *N*-glycosylation pathway, *via* phosphomannomutase (PMM2); excess Man-6-P is catabolized by the residual MPI activity (**Scheme 1**). Patients on this therapy survive and lead a normal life without obvious side effects (2).

To model MPI-CDG and follow the effects of mannose therapy, we previously knocked out the single *Mpi* gene in mice, leading to death at embryonic day 11.5 (E11.5) due to abnormalities in both placenta and the embryo. Mannose could not rescue because Man-6-P accumulates to toxic levels, limiting ATP and inhibiting several glycolytic enzymes (3). However, because patients with MPI-CDG have residual enzymatic activity, hypomorphic mice would offer a more patient-relevant model than would a complete *Mpi* knockout (KO). Here, we describe a viable, hypomorphic mouse line containing a patient-derived mutation that reduced enzymatic activity and altered mannose metabolism, as predicted. While a minority of mutant embryos died *in utero*, surprisingly, adolescent and adult mice had none of the expected symptoms reported in patients with MPI-CDG; these *Mpi*-deficient mice had a subclinical phenotype. However, if dams consumed mannose during pregnancy, most of the *Mpi* hypomorphic embryos died, and nearly half of the survivors were born with severe ocular defects. The combination of reduced enzymatic activity and the increased mannose load altered its metabolic flux, leading to Man-6-P accumulation in the eyes.

Mannose is widely used as a "natural" treatment for urinary tract infections; this seemingly innocuous sugar may have a negative effect for some pregnant women. While the frequency of MPI-CDG is unknown, women at risk for having subsequent MPI-CDG children who intend to take mannose as a "prenatal therapy" may inadvertently cause other side effects.

MATERIALS AND METHODS

Materials

Most of the reagents were purchased from Sigma-Aldrich (St. Louis, MO, USA). Dulbecco's modified Eagle's medium (DMEM) with 1 mg/ml glucose was purchased from Corning Cellgro (Manassas, VA, USA).

Fetal bovine serum (FBS) was obtained from Hyclone Laboratories (Logan, UT, USA). [2-^{3}H]-mannose was procured from Perkin Elmer (Boston, MA, USA). Protease inhibitor cocktail was purchased from Roche Diagnostics (Indianapolis, IN, USA). Carrier-free recombinant human tumor necrosis factor α (TNF-α) and recombinant mouse α-1 antitrypsin (AAT) were purchased from Cell Sciences (Canton, MA, USA), and ICL, Inc. (Portland, OR, USA), respectively. *N,O-bis*-[trimethylsilyl]trifluoroacetamide (BSTFA) was procured from Thermo Scientific (Waltham, MA, USA). Z-fix and Bouin's solution for tissue fixation were obtained from Anatech, Ltd. (Battle Creek, MI, USA) and Ricca Chemical (Arlington, TX, USA), respectively. Protein was measured by using the Pierce BCA protein estimation kit from Thermo Scientific.

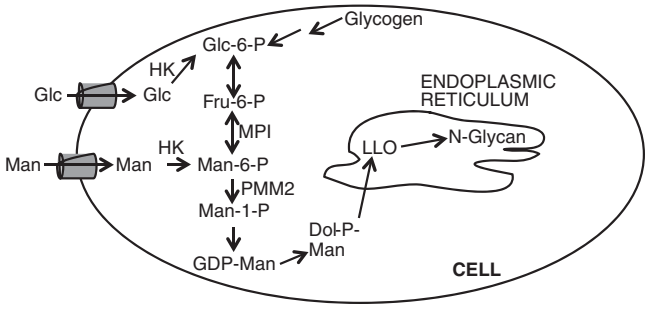

Scheme 1. Mannose metabolic pathway. Man, mannose; Glc, glucose; HK, hexokinase; MPI, phosphomannose isomerse; PMM2, phosphomannomutase2; GDP-Man, GDP-mannose; Dol-P-Man, dolichol phosphate mannose; LLO, lipid linked oligosaccharide.

Primers and probes

Primers were synthesized by Integrated DNA Technologies (San Diego, CA, USA). The following sequences were used. Primers: M14a-F1, GTAGGCCAGTGGACTAATGAAGCG; FnFL-F3, ATGGCCGCTTTTCTGGATTCA; LoxP-R1, CCTCAGCCCAAGCACCCAAATA; LoxP-F1, CCTTAGCTCCTTGCCCGACTGG. Probes for Southern blot: 5′ probes P717_01, GCAGGTGCCTGTGGAGGTCAG, and P717_02, CTTGTTAGGGGTGCCTGGATAGA; 3′ probes P717_03, GTGCGGCCATGTCCC TAACT, and P717_04, GATGTCCCCTGAACTGATTGTCTT.

Antibodies

Antibodies used in this study include antisera against AAT from Siemens (Marburg, Germany), chicken anti-mouse AAT IgY from ICL, and alkaline phosphatase-conjugated goat anti-chicken IgY IgG from Jackson ImmunoResearch (West Grove, PA, USA). The MPI-specific antibody was raised in our laboratory and has been described previously (4). The AP-2 antibody was obtained from the Developmental Studies Hybridoma Bank and was developed under the auspices of the U.S. National Institute of Child Health and Human Development and maintained by the University of Iowa Department of Biological Sciences (Iowa City, IA, USA). Antibodies against Brn3a, S-opsin, and M/L-opsin were purchased from Chemicon International, Inc. (Temecula, CA, USA). The anti-Pax6 antibody was purchased from Santa Cruz Biotechnology (Dallas, TX, USA). The secondary antibodies were purchased from Molecular Probes, Inc. (Eugene, OR, USA).

Animals

The Sanford-Burnham Medical Research Institute (SBMRI) Institutional Animal Care and Use Committee approved all the animal studies. $Mpi^{Y255C/Y255C}$ double knock-in (KI/KI) mice were created in C57BL/6J strain. $Mpi^{+/+}$ wild-type (WT) animals obtained from heterozygous $Mpi^{Y255C/+}$ crosses were used as controls. KI/KI animals were then crossed with mice heterozygous for the *Mpi*-KO allele ($Mpi^{+/-}$) on a mixed background (C57BL/6J and 129/SvEV) to create $Mpi^{Y255C/-}$ (KI/KO) mice. All the mice were maintained on a 12-h dark-light cycle.

Genotyping of mice

Genomic DNA was extracted from tail clips, and PCR was performed to confirm the genotype using primers M14a-F1

and LoxP-R1. Hotstart *Taq* Blue Mastermix (Denville Scientific, Inc., Metuchen, NJ, USA) was used for the amplification with the following cycle conditions: 94°C for 15 min for hotstart; 30 cycles of 94°C for 30 s, 60°C for 30 s, and 72°C for 1.5 min; and 72°C for 5 min at the end of 30 cycles. On 2% agarose gel, WT mice showed a 650-bp band, KI/KI mice showed a 750-bp band, and heterozygous mice showed both the bands (Supplemental Fig. S1*C*).

Isolation of murine embryonic fibroblasts (mEFs)

mEFs were isolated from KI/KI embryos at E11.5 as described previously (3). No additional mannose was required to propagate these mEFs.

^{3}H-mannose injection

[2-^{3}H]-mannose (50 μCi) was injected in the tail vein of 3 mice/group (WT, KI/KI, and KI/KO). Blood (20–30 μl) was collected at 5, 15, 30, 60, 90, 120, and 180 min, diluted with phosphate-buffered saline (PBS) and centrifuged at 1000 rpm. Diluted plasma was used to estimate the amount of ^3H_2O, [2-^{3}H]-mannose, and trichloroacetic acid (TCA) precipitable labeled glycoproteins. After 3 h, the mice were humanely euthanized, and their organs were collected.

Analysis of plasma ^3H_2O

A 10-μl aliquot of plasma was used to determine radioactivity with and without evaporation to dryness. The difference was defined as the amount of ^3H_2O in 10 μl of blood (5).

Analysis of plasma [2-^{3}H]-mannose

Free [2-^{3}H]-mannose in the plasma was determined by using HK and recombinant human MPI to convert it to ^3H_2O, before evaporating it. The difference between the radioactivity level before and after evaporation was defined as the amount of [2-^{3}H]-mannose in plasma (5).

Precipitation of plasma proteins

A 20-μl aliquot of plasma was diluted to 200 μl with PBS, and an equal volume of 20% TCA was added. The samples were incubated on ice for 1 h and centrifuged at 14,000 *g* for 15 min. The protein pellet was washed once with acetone and resuspended in 0.2 N sodium hydroxide. The amount of ^{3}H radiolabel in the precipitated protein was determined.

Stable isotope label

The cells were labeled with stable isotopes [1,2-^{13}C]-glucose and [4-^{13}C]-mannose, and isolated glycans were analyzed by gas-chromatography-mass spectroscopy (GC-MS) as described before (6).

Enzymatic activity assays

A small section of each organ to be tested was minced and disrupted by sonication in chilled 50 mM HEPES buffer (pH 7.4) containing protease inhibitors. Tissue lysate was centrifuged at 14,000 g for 10 min at 4°C. The supernatant was collected, and the amount of protein was measured by using the Pierce BCA protein estimation kit. A 15-μg aliquot of protein was used to estimate MPI activity. A standard coupled assay using phosphoglucose isomerase (PGI) and glucose-6-phosphate dehydrogenase (G6PD) with NADPH readout at 340 nm was used to estimate MPI activity in the organ lysate (7). The original protocol was modified to a final volume of 210 μl, and enzyme activity was measured in a 96-well plate for 2 h using a microplate reader (SpectraMax Plus^{384}; Molecular Devices, Sunnyvale, CA, USA).

Western blot analysis

A total of 50 μg of organ lysate (as described above) was separated by 12% SDS-PAGE and transferred to a nitrocellulose membrane. Unbound sites were blocked overnight at 4°C with PBS containing 5% bovine serum albumin (BSA). The membrane was probed with primary anti-mouse MPI diluted in PBS/2% BSA for 1 h at room temperature, followed by three 10-min washes, and then probed with horseradish peroxidase (HRP)-conjugated anti-rabbit secondary antibody at 1:2000 dilution in PBS/2% BSA for 1 h at room temperature. After 3 washes, the blot was developed by using BCIP substrate for HRP.

Blood/serum analysis

Glucose levels were determined by using FreeStyle glucometer and glucose strips from Abbot (Alameda, CA, USA). Several comprehensive parameters of freshly drawn blood were measured by using the VetScan VS2 instrument (Abaxis, Union City, CA, USA). Hematocrit analysis was done by using a VetScan HM2 analyzer (Abaxis).

Fecal AAT estimation

Fecal extracts were prepared as described previously (8), and AAT was measured by noncompetitive ELISA. Briefly, 96-well plates were coated with 100 μl of diluted antisera against human AAT, blocked with 1% BSA, washed with PBS, and incubated with 100 μl of fecal extract (diluted 1:50 with PBS) or standards; all steps were performed for 1 h at 37°C. Wells were washed with PBS and incubated with 100 μl of 0.4 μg/ml primary chicken anti-mouse AAT IgY prepared in 1% BSA and 0.05% Tween 20 for 18–24 h at 4°C. After washes with 0.05% Tween in PBS, wells were incubated with 100 μl of 0.25 μg/ml alkaline phosphatase-conjugated goat anti-chicken IgY prepared in 1% BSA and 0.05% Tween 20 for 2 h at 37°C. This was followed by washes and color development using 4-nitrophenyl phosphate as substrate. Absorbance was measured at 405 nm using a microplate reader (SpectraMax Plus^{384}; Molecular Devices). The amount of fecal AAT (ng/ml, feces extract) was derived from standard curve and reported as mean micrograms AAT per gram of dried stool.

Serum mannose determination by GC-MS

Mannose was estimated by using a previously described method (9). Briefly, 10-μl serum and mannose standards were derivatized by addition of 50 μl hydroxylamine hydrochloride (50 mg/ml) in 1-methyl imidazole and incubation at 65°C for 30 min. Then, 100 μl acetic anhydride was added. Extraction was done with 100 μl chloroform and 200 μl water. After vortexing and centrifuging the samples, the aqueous layer was removed and reextracted once more with water. The chloroform layer containing sugars was dried and solubilized in chloroform for GC-MS analysis (GCMS-QP2010 Plus; Shimadzu, Kyoto, Japan).

In vivo imaging of embryos *in utero*

Timed matings were set up for WT and KI/KI mice supplemented with 5% mannose in their drinking water. Females

were checked for the presence of a vaginal plug the following morning to confirm the mating. The Vevo 770 (VisualSonics, Toronto, Canada) *in vivo* microimaging system was used with the RMV scan heads 708 and 703 at a center frequency of 55 and 35 MHz, respectively, to visualize embryos in pregnant mice starting at E6.5.

Histological examination of the tissues

Freshly dissected tissues or embryos were immediately fixed in buffered zinc-formalin, Z-fix. Bouin's solution was used to fix the entire head with eyes after birth. Paraffin-embedded sections (5 μm thick) were cut and then stained with hematoxylin and eosin (H&E) for structural analysis using the Aperio Scanscope slide-scanning system (Aperio Technologies, Inc., Vista, CA, USA). Morphometric measurements were performed with Aperio Imagescope software.

Immunohistochemistry

The sections were deparaffinized, and antigen retrieval was performed in 0.01 M sodium citrate for 30 min. Permeabilization was done with 1% saponin. The sections were blocked with 10% normal goat serum (for Brn3a, S-opsin, and M/L-opsin) or 10% donkey serum (for Pax6 and AP-2) and incubated overnight at 4°C with the following diluted primary antibodies: Brn3a (1:10), S-opsin and M/L-opsin (1:200), Pax6 (1:100), and AP-2 (1:10). Next, fluorescently tagged secondary antibody was added. After a thorough washing, Vectashield (Vector Laboratories, Burlingame, CA, USA) was added, and sections were sealed with a coverslip. Confocal images (size 1024×1024) were obtained sequentially on a Zeiss 710 Laser Scanning Confocal System (Carl Zeiss, Oberkochen, Germany) using either a ×20/0.80 NA WD 0.55 objective lens or EC Plan-Neofluor ×40/0.75 M27 objective lens. Results were confirmed using 3 different biological samples. Quantification consisted of using ImageJ software (U.S. National Institutes of Health, Bethesda, MD, USA) to count the number of immunopositive cells in 2 different confocal images (1024×1024 taken at ×40) of the posterior region of 3 different eyes.

Man-6-P assay

The embryo, placenta, and eye extracts were prepared as previously published (10). The method for Man-6-P estimation was modified from a protocol originally designed for glucose-6-phosphate (Glc-6-P) estimation (11). We used a coupled enzyme assay, which uses MPI, PGI, and G6PD to convert Man-6-P to Glc-6-P, with a final fluorescence readout. This method was optimized and validated by estimating Man-6-P in the mixtures containing known amounts of Man-6-P, Fru-6-P, and Glc-6-P or adding known amounts of Man-6-P to tissue lysates. The values obtained by this method were comparable to the results obtained by using fluorophore-assisted carbohydrate electrophoresis (FACE; refs. 12, 13). Briefly, 20 μl tissue extract of each sample type was dispensed in different wells of a black assay plate. Depending on the number of samples, 2 sets of reaction mix were prepared containing 50 mM HEPES, 1 mM magnesium chloride, 100 μM NADP, 10 μM resazurin, and 0.25 U diaphorase in a total volume of 80 μl/sample. MPI, PGI, and G6PD (0.25 U/sample) were added to one set (F_3) and only G6PD and PGI (0.25 U/sample) were added to the other set (F_2). Another mix containing G6PD, but devoid of NADP, was prepared to determine the background (F_b) due to the endogenous NADP in each sample. An 80-μl aliquot of the mix was added to the wells containing 20 μl of the extract. After 15 min, fluorescence was recorded at excitation wavelength 530 nm and emission at 590 nm using Flexstation III (Molecular Devices). Background fluorescence F_b was subtracted from all the samples (F_3 and F_2). Difference between the fluorescence values ($F_3 - F_2$) was used to calculate picomols of Man-6-P using a standard curve generated with known amounts of Glc-6-P in 20 μl deionized water and 80 μl reaction mix containing G6PD.

GC-MS analysis of metabolites in the eyes

The eyes were crushed and washed once with cold PBS. Then, 100 μl chilled 0.1 M acetic acid with 3 nmol arabitol (internal standard) was added to the tissue, and the mixture was sonicated briefly on ice. The samples were centrifuged at 8000 *g* for 5 min in a cold centrifuge, and the supernatant was collected. Extraction was repeated once more, and the supernatants were combined. The extract was lyophilized, derivatized with hydroxylamine hydrochloride and BSTFA, and subjected to GC-MS (GCMS-QP2010 Plus; Shimadzu) according to a method as modified from Halket and Zaikin (14).

Vision test

Optokinetics was measured by using an optometer with motorized drum painted with black and white strips, which was built in-house at The Scripps Research Institute (La Jolla, CA, USA). The measurements were done under photopic conditions with light intensity of 150 lux. The mouse was placed on the wire mesh inside the drum and allowed to acclimate for 5 min without rotation and then for 30 s with rotation. The drum rotation (2 rotations/min) went clockwise for 1 min and then continued anticlockwise for 1 min with an interval of 30 s between the rotations. The animals with normal vision followed the movement of the rotating drum, whereas the ones with impaired vision failed to track the drum rotations. The visual response was measured by recording the number of head turns during drum rotations.

RESULTS

Selection of MPI mutation

Since patients with MPI-CDG have 3–20% residual MPI activity (1), we wanted to make a hypomorphic mouse line with similar residual activity to model the disorder and test mannose therapy. To identify a candidate, 8 mutations from patients with confirmed MPI-CDG were introduced into the mouse *Mpi* gene to obtain the following amino acid changes: S102L, D131N, M138T, R152Q, R219Q, Y255C, I398T, and R418H. Subsequently, mutant MPI constructs were expressed in *mpi*-null yeast strain SEY6210delpmi40::URA3, and activity was determined (**Table 1**). Mutation Y255C (TAC→TGC) retained ~12% activity (Table 1), which was confirmed by expression in CHO, COS7, and $Mpi^{-/-}$ mEFs and consistently had 8–14% activity (data not shown). Y255C was selected to generate a KI mouse line, as described in Supplemental Fig. S1.

Hypomorphic mice have modest embryonic lethality

Both $Mpi^{Y255C/Y255C}$ (KI/KI) and $Mpi^{Y255C/-}$ (KI/KO) mice were viable. Heterozygous crosses (KI/+ × KI/+)

TABLE 1. *MPI residual activity and antigen in* mpi-*null SEY6210delpmi40::URA3 yeast strain complemented with mutant* mpi *constructs*

MPI mutation	Residual MPI protein (%)	Residual MPI activity (%)
WT	100	100
S102L	0	0.59
D131N	0	7.3
M138T	53.0	82.4
R152Q	83.1	99.7
R219Q	58.7	38.7
Y255C	24.9	12.3
I398T	101.2	109
R418H	66.2	65.3

showed a small, but significant (P=0.004), decrease of 16% below the expected number of KI/KI animals, indicating modest embryonic lethality (**Table 2**). Similarly, homozygous (KI/KI × KI/KI) crosses produced litters that were significantly (P=0.01) smaller than WT animals [WT: 8.6 (n=46) *vs.* KI/KI: 7.5 (n=33)]. KI/KI survivors had normal weight gain (Supplemental Fig. S2) and life span, showing no visible abnormalities in the organs as monitored by dissections at different times up to 13 mo (data not shown).

Hypomorphic mice have reduced MPI activity and protein in various organs

KI/KI mice were predicted to have ~8–14% residual MPI activity and KI/KO mice ~4–7% activity compared with WT. **Table 3** shows the result of enzymatic assays of different organ lysates. In KI/KI mice, the enzyme activity was reduced to ~18% in heart and nearly 2–3% in small intestine and liver (**Fig. 1*A***). KI/KO small intestine and liver had 4- and 6-fold lower MPI activity, respectively, than those of KI/KI (Fig. 1*A*). Assays of mixed extracts of different organs showed no evidence for the presence of inhibitors or activators. Despite these unexpected low activities in liver and small intestine, all mutant animals appeared to be healthy, and none had any abnormal hepatointestinal pathological features on histochemical analysis (data not shown). Residual MPI protein antigen ranged from 25 to 45% in various tissues from KI/KI mice and 14 to 33% in KI/KO mice (Fig. 1*B*). Our results clearly demonstrate reduced MPI protein and enzyme activity in hypomorphic mice, similar to that in fibroblasts and leukocytes of patients with MPI-CDG (1).

TABLE 2. *Heterozygous crosses [KI/+ × KI/+]*

Parameter	Genotype		
	WT (+/+)	Het (KI/+)	KI/KI
Mice (n)	133	303	115
Predicted (%)	25	50	25
Observed (%)	24.1	54.9	20.8
P	0.187	0.830	0.004

Data from 70 litters. Het, heterozygous.

TABLE 3. *MPI specific activity in various organs*

Organ	Activity (nmol/mg/min)		
	WT	KI/KI	KI/KO
Embryo, E11.5	24.6 ± 1.6	1.6 ± 0.32	ND
Placenta, E11.5	22.1 ± 6.9	1.5 ± 0.15	ND
Small intestine	20.5 ± 0.6	0.51 ± 0.29	0.14 ± 0.20
Kidney	19.7 ± 0.9	1.20 ± 0.14	0.57 ± 0.08
Colon	16.8 ± 2.7	1.46 ± 0.53	0.92 ± 0.18
Heart	14.9 ± 2.1	2.80 ± 0.6	1.4 ± 0.01
Liver	8.3 ± 0.9	0.25 ± 0.03	0.04 ± 0.005
Lung	8.4 ± 2.3	0.68 ± 0.21	0.32 ± 0.18
Spleen	7.5 ± 0.2	0.42 ± 0.15	0.28 ± 0.06
Eye	1.5 ± 0.2	0.12 ± 0.02	ND

Data are means ± SD of n = 3 mice. ND, not determined.

Reduced MPI alters mannose flux in hypomorphic mice

Reduced MPI activity is predicted to increase mannose flux toward glycoprotein synthesis and decrease its catabolism (6). To confirm this, we labeled mice, organ cultures, and mEFs with [2-^{3}H]-mannose and measured label incorporation into glycoproteins and catabolic production of ^3H_2O ([2-^{3}H]-mannose→[2-^{3}H]-Man-6-P→Fru-6-P+^3H_2O). Reduced MPI should increase label incorporation into proteins and decrease catabolism of [2-^{3}H]-mannose to ^3H_2O (Scheme 1). As seen in **Fig. 2*A***, KI/KI mEFs incorporated 5-fold more [2-^{3}H]-mannose into glycoproteins than did WT, similar to the phenomena seen in the fibroblasts of patients with MPI-CDG (Fig. 2*B*). Compared with WT mice, KI/KI and KI/KO mice injected with 50 μCi [2-^{3}H]-mannose in the tail vein had a reduced rate of production of ^3H_2O in serum (Fig. 2*C*) together with a 5- to 6-fold increase in [2-^{3}H]-mannose incorporation in serum glycoproteins (Fig. 2*D*). Labeling of organ explants *ex vivo* showed 2- to 6-fold higher incorporation of [2-^{3}H]-mannose in glycoproteins from KI/KI organs (Fig. 2*E*), levels similar to those of mEFs and MPI-CDG patient fibroblasts (Fig. 2*A*, *B*). We also labeled mEFs from WT and KI/KI mice with the stable isotopes [1,2-^{13}C]-glucose and [4-^{13}C]-mannose under physiological conditions of 5 mM glucose and 50 μM mannose. Mannose directly contributed ~25% of mannose to WT N-glycans. This contribution increases by 2.3-fold to 57% in KI/KI mEFs with reduced MPI activity (data not shown). These results show that *Mpi* hypomorphic mice clearly have altered mannose metabolic flux due to the decreased activity.

Since the biochemical difference between KI/KI and KI/KO mice was small, only KI/KI mice on the pure C57BL/6J background were used in subsequent experiments.

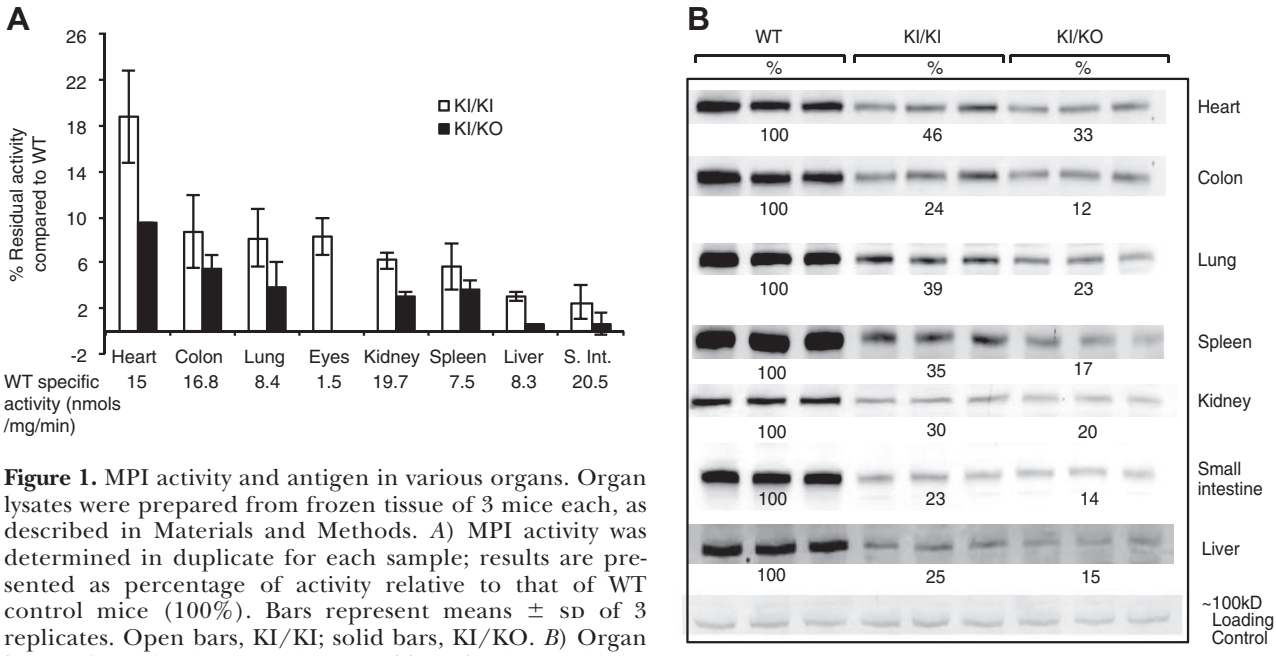

Figure 1. MPI activity and antigen in various organs. Organ lysates were prepared from frozen tissue of 3 mice each, as described in Materials and Methods. *A*) MPI activity was determined in duplicate for each sample; results are presented as percentage of activity relative to that of WT control mice (100%). Bars represent means ± SD of 3 replicates. Open bars, KI/KI; solid bars, KI/KO. *B*) Organ lysates from 3 mice were immunoblotted using anti-MPI antibody. Percentages represent intensity of KI/KI and KI/KO protein bands relative to that of WT, as calculated by ImageJ software.

KI/KI mice do not mimic MPI-CDG symptoms despite altered mannose metabolism

Patients with MPI-CDG are often hypoglycemic and have elevated serum alanine transaminase (ALT) and aspartate aminotransferase (AST) indicating liver pathology. They also have hypoalbuminemia and low antithrombin III (ATIII) levels and liver fibrosis, and some have intestinal villus atrophy and protein-losing enteropathy (PLE).

We comprehensively analyzed serum from WT and KI/KI mice aged 3 and 10 mo. No major differences existed in serum parameters of WT and KI/KI mice at any age (data not shown). KI/KI mice have normal glucose and liver enzymes. Potassium, an indicator of renal function, was significantly (P=0.01) higher in KI/KI animals (7.5 mM) than in WT (7.05 mM) but was still within the normal range for mice. KI/KI mice had normal kidney function with no evidence of either proteinuria or increased blood urea nitrogen (BUN) concentration. The results of hematocrit analysis did not show any difference in the numbers of various blood cells, except for slight but significant (P=0.02) decrease in red blood cells of KI/KI mice ($10.8\pm 0.2\times10^{12}$/L) from that in WT mice ($11.06\pm0.1\times10^{12}$/L). However, this decreased amount was within the normal range for mice. Lysosomal enzymes, aspartyl glucosaminidase (AGA) and β-hexosaminidase (β-hex) are elevated in patients with CDG-I (15), but in *Mpi* hypomorphic mice, these activities (AGA: 9.7±0.77 nmol/h/ml; β-hex: 33.4±4.5 nmol/min/ml) were no different from WT (AGA: 10.5±0.73 nmol/h/ml; β-hex: 36.2±8.3 nmol/min/ml). Plasma proteins, such as transferrin and AAT, and coagulation factors, such as antithrombin III and factor XI, are affected in patients with MPI-CDG (16), but they were unaltered in KI/KI mice, based on Western blots (data not shown). Histological analysis of various organs, including liver and intestine at 3, 5, 7, and 13 mo, showed no morphological changes (data not shown), confirming that no visible pathology was present even in older mice. Because some patients with MPI-CDG have PLE (*i.e.*, loss of plasma proteins through small intestines), we also determined enteric protein loss in WT and KI/KI mice by measuring fecal AAT. KI/KI mice had neither enhanced levels of fecal AAT at basal state nor increased susceptibility to enteric protein loss when systemically challenged with TNF-α, which is known to increase intestinal permeability (ref. 17 and Supplemental Fig. S3). Our observations demonstrate that, despite having altered mannose metabolism and reduced MPI activity levels similar to those of patients with MPI-CDG, KI/KI mice failed to mimic any of the expected MPI-CDG symptoms.

Effects of mannose supplements

There was a small but significant reduction in the number of KI/KI pups from heterozygous breeding (Table 2). We assumed that this was due to impaired glycosylation during embryogenesis and that the lethality would be rescued by providing mannose to the dams in their drinking water. Providing mice with 1% (w/v) mannose in their drinking water (60–80 mg/100 g body weight/d) is equivalent to the therapeutic doses given to patients with MPI-CDG (80–100 mg/100 g body weight/d). We supplied 0, 1, 2, and 5% mannose in the drinking water of WT and KI/KI dams and also to 6- to 8-wk-old mice.

Supplementing 1–5% mannose in the drinking water of 6- to 8-wk-old hypomorphic mice had no obvious ill

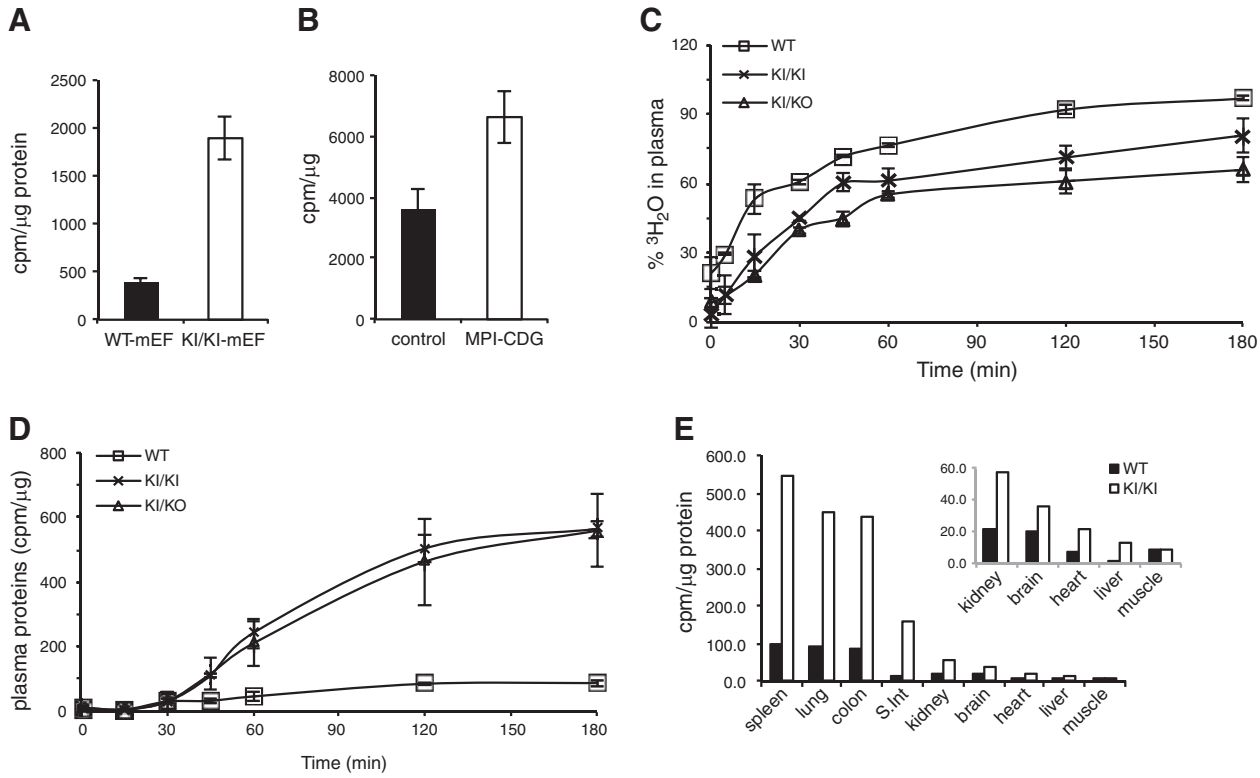

Figure 2. [2-^{3}H]-mannose labeling of fibroblasts and mice. *A*, *B*) Fibroblasts from mouse embryos (*A*) or human fibroblasts (*B*) were labeled in duplicate with [2-^{3}H]-mannose, and radiolabel was measured in TCA-precipitable proteins. Mice were injected with 50 μCi [2-^{3}H]-mannose, and blood was collected at different times. *C*, *D*) Calculated ^3H_2O (*C*) and TCA-precipitable ^{3}H-radiolabeled glycoproteins (*D*). Data represent means of 3 mice/group. Error bars = SD. *E*) Organ explants from WT and KI/KI mice were labeled with 50 μCi/ml [2-^{3}H]-mannose, and radiolabel was measured in glycoproteins precipitated with TCA. Inset: magnified view of the selected organs.

effects for over 4–6 mo. They were healthy and grew normally, confirming that there were no toxic effects of mannose therapy, which is also consistent with results in human studies. However, providing mannose to dams was lethal to the developing embryos. Crossing heterozygous KI/+ mice did not produce any KI/KI progeny when dams drank water containing 5% mannose (**Table 4**). Crossing homozygous KI/KI mice gave the same results. Ultrasound analysis of the dams showed that implantation occurred, but embryos were resorbed over time (**Fig. 3**). Dissections at E13.5 revealed normal development of WT embryos (**Fig. 4*A*, *B***) and abnormal hemorrhaged placenta and resorbed embryos for KI/KI (Fig. 4*C*). The results of histology analysis also showed a grossly disorganized placenta with a labyrinth layer devoid of blood vessels and embryonic erythrocytes, abnormally organized giant cells, and an expanded spongiotrophoblast (Fig. 4*D*, *E*).

KI/KI dams supplemented with 1 and 2% mannose produced live offspring, but litter size was significantly smaller than that of WT controls. Extensive placental hemorrhage occurred in the 5% mannose-supplemented group but not in the 2% mannose-fed KI/KI dams. However, placental size was significantly smaller than WT at various embryonic stages (**Fig. 5*A***). Sectioning of intact uteri bearing embryos (E8.5) showed developmental delay and abnormalities in KI/KI embryos that were not present in age-matched WT em-

TABLE 4. *Heterozygous breedings with mannose supplementation*

	Heterozygous cross and progeny genotype					
	KI/+ × KI/+, no mannose			KI/+ × KI/+, 5% mannose		
Parameter	+/+	KI/+	KI/KI	+/+	KI/+	KI/KI
Average litter size	8.0 ± 1.7, n = 14			6.0 ± 2.3, n = 6		
Survival to weaning (%)	84.8			94.4		
Progeny (n)	29	49	17	14	20	0
Progeny (%)	31	52	18	41	59	0
P	0.26	0.26	0.04	0.12	0.44	–

Data are means ± SD; n = number of litters.

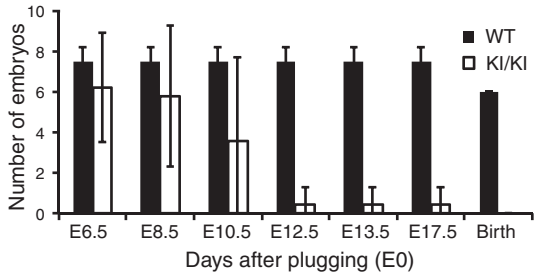

Figure 3. Embryo survival. Timed matings were set up, and dams were provided with 5% mannose in drinking water during gestation. *In vivo* imaging was performed to monitor pregnancies. Bars represent means ± SD of 5 experiments.

bryos (Fig. 5*B*, *C*). These affected embryos would eventually die before birth.

The results here clearly show adverse effects of mannose supplementation on both placentas and embryos. Dams continued nursing on 1 or 2% mannose during weaning, but pup survival showed a dramatic dose-dependent decrease *vs.* controls (**Table 5**). The causes of death could not be investigated, because most pups were reported as missing (most likely, cannibalized by the mother).

Man-6-P accumulates in KI/KI embryos and placentas from dams drinking mannose-supplemented water

KI/KI mice given 1 and 2% mannose supplements significantly increase plasma mannose by 1.3- to 1.5-fold compared with mannose levels of those given plain water (**Fig. 6**). WT mice also showed a 50% increase in mannose levels with 2% mannose, which is consistent with the results of earlier studies (18, 19).

At E11.5, MPI specific activities in placental and whole-embryo lysates of KI/KI mice were 6–7% of those in WT (Table 3). None of the organs from WT or KI/KI adult mice supplemented with mannose showed significant Man-6-P accumulation (data not shown). In contrast, baseline Man-6-P was higher in both KI/KI placentas and embryos compared with that in WT. There was an additional increase by ~2.5 fold on 1–2% mannose supplementation (**Fig. 7**). Man-6-P content in the embryos of WT dams supplemented with 2% mannose was comparable to that of KI/KI mice without mannose, and neither group showed any ill effects. Our previous studies on *Mpi*-null mice show that increased Man-6-P can cause ATP depletion and death (3).

However, ATP levels of E11.5 embryos and placentas from mannose-supplemented KI/KI and WT dams were similar (data not shown).

Mannose-supplemented KI/KI mice have eye defects

Effect of mannose supplementation during conception and gestation

Surviving KI/KI pups born to mannose-fed dams and subsequently maintained on mannose had normal growth and life span. There were no visible abnormal-

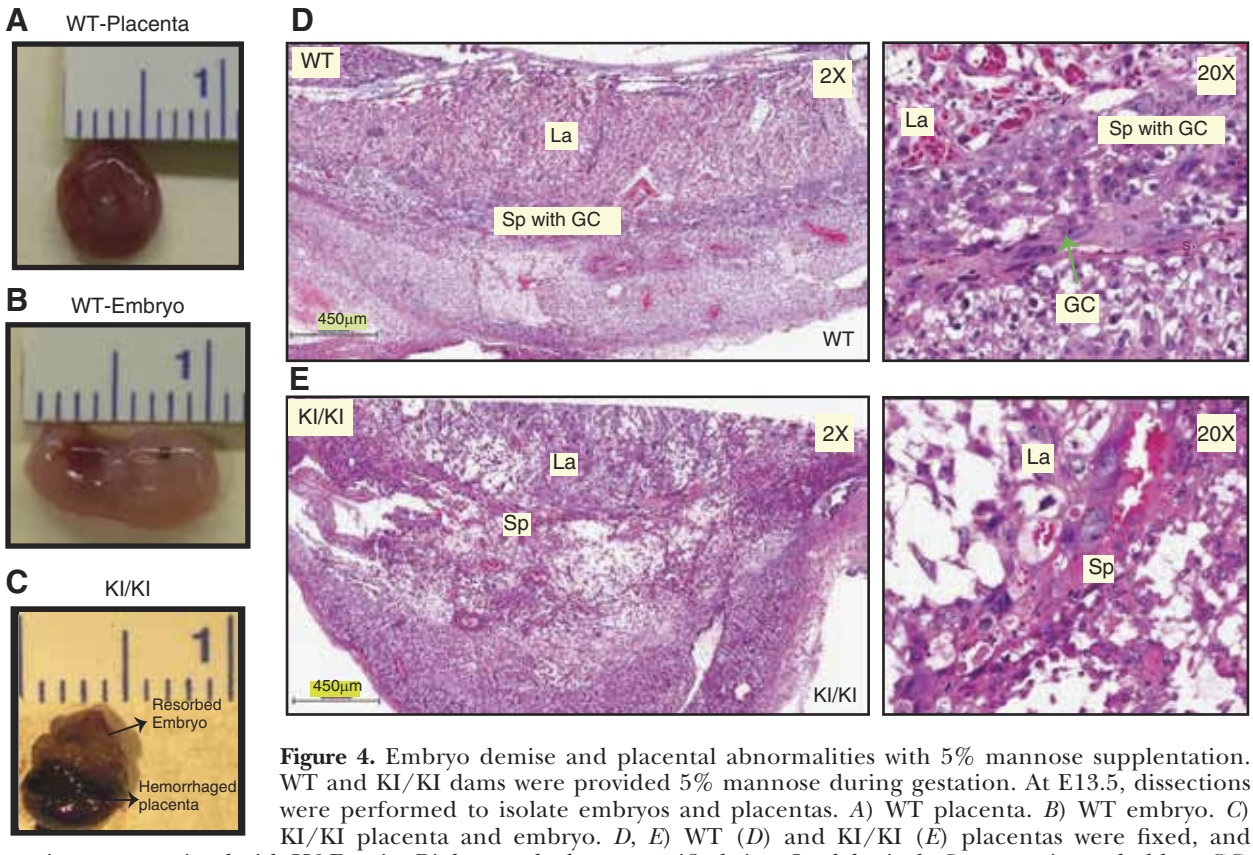

Figure 4. Embryo demise and placental abnormalities with 5% mannose supplentation. WT and KI/KI dams were provided 5% mannose during gestation. At E13.5, dissections were performed to isolate embryos and placentas. *A*) WT placenta. *B*) WT embryo. *C*) KI/KI placenta and embryo. *D*, *E*) WT (*D*) and KI/KI (*E*) placentas were fixed, and sections were stained with H&E stain. Right panels show magnified view. La, labyrinth; Sp, spongiotrophoblast; GC, giant cells.

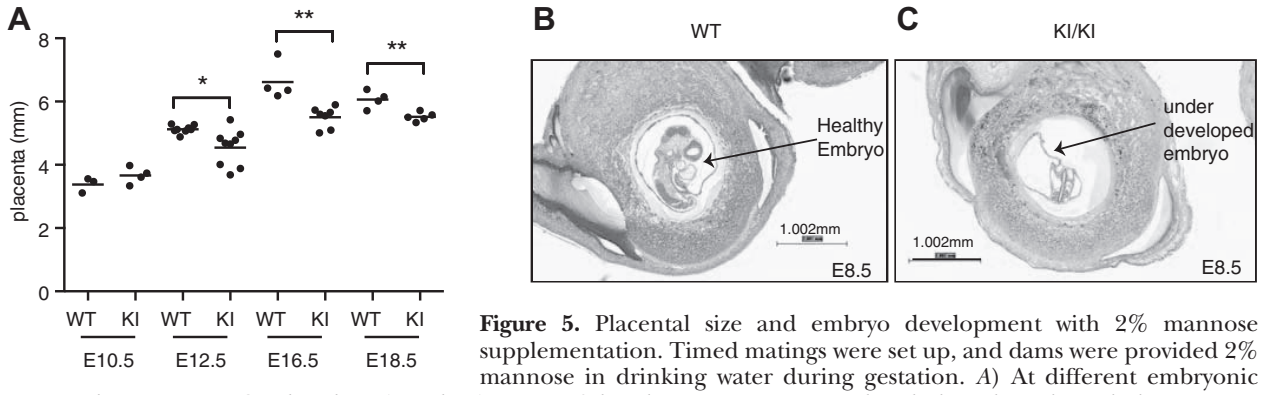

Figure 5. Placental size and embryo development with 2% mannose supplementation. Timed matings were set up, and dams were provided 2% mannose in drinking water during gestation. *A*) At different embryonic stages, placentas were fixed and sectioned. Diameter of the placenta was measured and plotted. Each symbol represents an individual placenta. *B, C*) At E8.5, whole WT (*B*) and KI/KI (*C*) uteri were fixed, and sections were stained with H&E to visualize embryos *in utero*. $*P < 0.05$, $**P < 0.005$.

ities in any organ when KI/KI mice were dissected and compared with WT. The eyes were checked every week starting at wk 2, when the mice just opened their eyes, and continuing for up to 8 mo. Approximately 45% of mannose supplemented pups displayed severe morphological eye defects (**Table 6**) that were clearly evident 2–8 wk after birth. Most of the affected pups had either cloudy/opaque eyes (**Fig. 8*B***) or no eyes that appeared as shuteye (Fig. 8*C*) compared with normal eyes (Fig. 8*A*). Histological analysis was done on the adult eyes isolated at 8 mo. WT eyes showed normal development of all eye structures including lens, retinal-pigmented epithelium (RPE), and retina (Fig. 8*D*). KI/KI mice that developed obvious eye defects by 3 wk of age showed smaller eyecups, absence of the lens, disorganized retina, and clustering of pigmented cells inside the eyecup (Fig. 8*E*). Mice with shuteye developed much smaller eyecups and had extensive hemorrhage, with no eye structure remaining except for an eye socket-like structure containing pigmented tissue with vacuoles (Fig. 8*F, G*). The identity of these cells is unknown, but markers for RPE progenitors, Mitf and Otx2, failed to stain the pigmented mass (data not shown). One KI/KI mouse supplemented with mannose since conception had a defective right eye and a seemingly normal left eye. However, when euthanized at 8 mo, the left eye also had a degenerating lens (Fig. 8*H*).

Effect of mannose on postnatal eye development in KI/KI mice

Since eye development continues up to 4 wk postbirth, we supplemented KI/KI mice with 1 or 2% mannose after birth, starting at P1, where the development of the eye and lens is expected to be normal till birth. However, this set of mice also showed eye defects with 2% mannose supplementation, some of which were observed by 3 wk; those exposed to 1% mannose did not (Table 6). The histological examination at 8 mo showed an eye with disintegrated lens, excess extracellular matrix (ECM), distorted retina, and accumulated pigmented cells (Fig. 8*I*), suggesting ill effects of P1 mannose supplementation. Some mice with mannose exposure also developed cloudy eyes later at ~3 mo, with clear signs of cataract and a deteriorating lens and retina (Fig. 8*J*). In this case, besides accumulation of ECM, the nucleus of the lens protruded out of the lens capsule and was vacuolated.

Vision of WT and KI/KI mice was checked by using an optometer with a motorized drum, painted with black and white strips. Mice with defective right eyes did not show any head turns during clockwise rotation, and the ones having defects in the left eye failed to show any head turns during counterclockwise rotation (Supplemental Table S1). Mice with both eyes affected did not show any head turns in either direction. These data confirmed that the eyes that developed defects either early on or later in life were functionally impaired. None of the KI/KI animals had eye defects when mannose was added to the drinking water at 6–8 wk of age, which is 2–4 wk after full eye development.

Our results here clearly suggest that mannose supplementation starting before conception or 1 d postbirth causes two separate, time-resolved types of eye

TABLE 5. *Homozygous breedings with mannose supplementation*

Mannose in drinking water (%)	Litters (*n*)		Average litter size (*n*)			Survival to weaning (%)		
	WT	KI/KI	WT	KI/KI	*P*	WT	KI/KI	*P*
0	46	33	8.6 ± 1.8	7.5 ± 2.0	0.01	90	84	0.13
1	8	17	8.0 ± 1.3	5.3 ± 1.0	0.01	92	61	0.001
2	11	9	9.6 ± 1.3	5.4 ± 3.9	0.005	84	33	0.02
5	3	5	6.7 ± 1.2	0.0	–	15	0.0	–

Average litter size data are means ± SD.

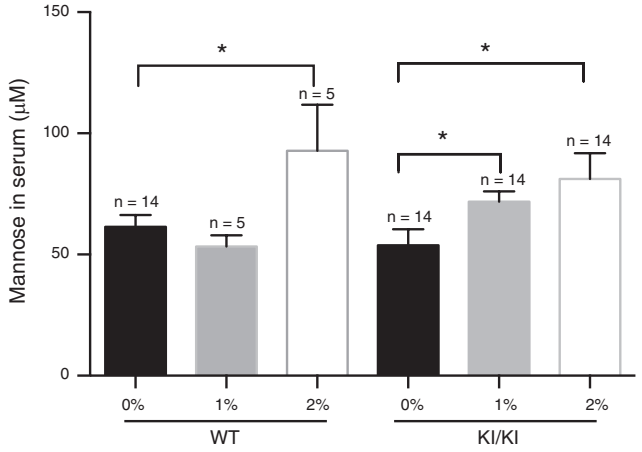

Figure 6. Serum mannose analysis. Concentration of mannose in serum from WT and KI/KI mice was determined by GC-MS, as described in Materials and Methods. $*P < 0.05$.

pathology in KI/KI mice, which seemed to be rooted in altered mannose metabolism.

Mannose initiates ocular defects during embryogenesis

We could observe the eyes once mice opened them ~2 wk. Eye development starts around E8.5 and continues until 4 wk postbirth. We wanted to know whether eye deterioration starts at embryonic stages or postbirth in mice exposed to mannose *in utero*. We provided 2% mannose in KI/KI dams' drinking water during timed matings and monitored embryonic eye development at various stages by histology. At E10–E11, WT mice develop an appropriate lens pit (**Fig. 9*A***), but KI/KI mice given mannose do not (Fig. 9*B*). Instead they form smaller lens vesicles at E12–E13 (Fig. 9*D*) or none at all (Fig. 9*E*). Wild-type mice had well-formed lenses at E12–E13 (Fig. 9*C*), and both WT and KI/KI mice formed a neuroepithelium and an outer layer of RPE. Some of the mannose-exposed eyes continued to develop with small lens vesicles or without any lens (E14–E15; Fig. 9*G*, *H*) when compared with WT (Fig. 9*F*). By E16–E17, WT eyes had a well-differentiated clear lens and a laminated retina with inner and outer layers (Fig. 9*I*). Eyes from mannose-exposed mice were much smaller and had a neuroepithelium that lagged behind in its differentiation and mesenchymal cells from the surrounding area, as well as blood cells that appeared to infiltrate the vacant area of the optic cup (Fig. 9*J, K*). By E18–E19, in some cases, the retina folded around in the vitreous space with an overproduction of retina cells and delayed differentiation. The optic cup of affected KI/KI eyes was significantly smaller than that of WT eyes at all embryonic stages (**Fig. 10**). Some of the mannose-supplemented mice were then born with eyes that had a small, deteriorating cataractous lens (Fig. 9*P*) or were devoid of lens (Fig. 9*Q*), and the optic cup was filled with different cell types, which further deteriorated with time (Fig. 8*E*, *G*).

We assessed the effects of mannose on retinal development by using a series of retinal cell type-specific antibodies. Pax6 served as an early marker for retinal progenitors during neurogenesis. After the onset of retinal differentiation, it indicates ganglion and amacrine cells. In addition, we could specifically detect ganglion cells (Brn-3a), amacrine cells (AP-2), and photoreceptors (S opsin and M/L opsin). We could detect ganglion cells present in the ganglion cell layer, amacrine cells present in the inner nuclear layer, and photoreceptors in the outer nuclear layer that expanded their outer segments next to the RPE at the back of the eye in WT and KI/KI eyes at P28 (**Fig. 11*A, B***). The number of Brn-3a$^+$ ganglion cells was not affected (Fig. 11*B*). However, there were significantly fewer AP-2-positive amacrine cells in the mature KI/KI eyes (Fig. 11*A*, *D*), as well as at embryonic stage E18.5 (Fig. 11*C*, *D*). Mannose may either partially impair differen-

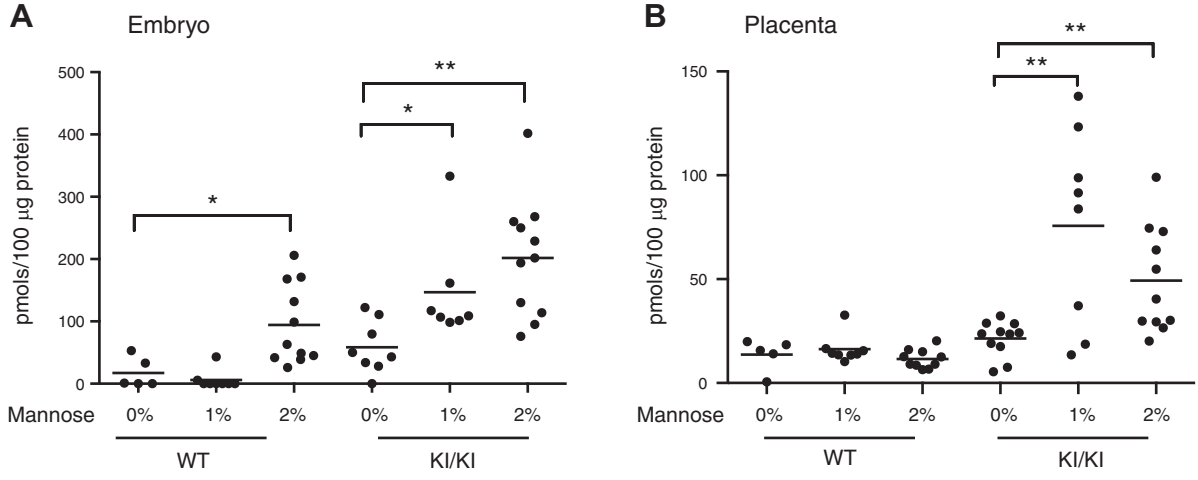

Figure 7. Man-6-P determination. Embryos (*A*) and placentas (*B*) were isolated at E11.5 from ≥2 different dams with or without mannose supplementation, and Man-6-P was determined. Each symbol represents an individual embryo/placenta. $*P < 0.05$, $**P < 0.005$.

TABLE 6. *Mannose-supplemented mice develop eye defects*

Mannose supplementation	WT			KI/KI				
					With eye defects (*n*)			
	Total (*n*)	With eye defects (*n*)	Affected (%)	Total (*n*)	Total	Early, 2–8 wk	Late, >8 wk	Affected (%)
Conception								
1%	55	1	1.8	49	23	16	7	46.9
2%	88	1	1.1	20	9	9	0	45.5
Postbirth (P1)								
1%	30	0	0	26	1	1	0	3.8
2%	36	0	0	20	9	5	4	45
6 wk								
1%	14	0	0	14	0	–	–	0
2%	14	0	0	14	0	–	–	0

tiation of normal retina progenitor cells to amacrine cells in KI/KI embryonic eyes or lead to their apoptosis.

Our results clearly demonstrate that mannose-induced eye abnormalities in KI/KI embryos begin early in embryogenesis, starting with impaired lens formation and subsequently differentiation of some retinal cells required for further eye development. The results of our statistical analyses (Table 6) and histological examination of the eyes suggest that there is a variable penetrance of *Mpi* eye pathology.

Affected eyes have elevated mannose and Man-6-P levels

Eyes have the lowest MPI specific activity of all organs tested, and this activity was reduced by 92% to 0.124 ± 0.025 nmol/min/mg in KI/KI animals (Table 3). Low MPI activity might render eyes more susceptible to adverse effects of mannose supplementation by accumulating Man-6-P. The Man-6-P content of the eyes was similar in WT and KI/KI mice without mannose supplementation (**Fig. 12*A***). However, it increased 1.3-fold in the normal appearing KI/KI eyes and by 2.0-fold in the visibly cloudy eyes in 1 or 2% mannose-supplemented KI/KI mice (Fig. 12*A*). We used GC-MS to check the levels of mannose, Man-6-P and mannitol in the affected and normal eyes of 1% mannose-supplemented KI/KI mice. Mannitol did not accumulate, but mannose and Man-6-P levels were significantly higher in the affected eyes than in the normal eyes (Fig. 12*B*). These results suggest that ongoing mannose consumption raises mannose and Man-6-P levels in KI/KI eyes and correlates with increased ocular abnormalities.

DISCUSSION

There are now 100 known types of human glycosylation disorders. The CDG group comprises most of them. One of the major hurdles in studying these disorders is the lack of animal model systems. Mouse and rat mammalian models are closely related to humans and are widely used to study inherited human disorders. A few attempts have been made in the past to create KO mouse models; however, the models for MPI-CDG (CDG-Ib), PMM2-CDG (CDG-Ia), SRD5A3-CDG (CDG-Iq), and DPAGT1-CDG (CDG-1j) are embryonically lethal (3, 20–22), and those for MGAT2-CDG (CDG-IIa), SLC35C1-CDG (CDG-IIc), and β4GalT1-CDG (CDG-IId) have early postnatal lethality (23–26). These outcomes emphasize the importance of glycosylation for early human development, but they cannot be used to model most aspects of the disease. Hypomorphic lines are more likely to mimic patient phenotypes.

We chose to create a murine line containing a mutation that generates a Y255C transition in MPI because preliminary experiments in cell lines showed that this line retains ~8–14% residual MPI activity. This amount of activity should ideally mimic residual activity seen in the patient who was a compound heterozygote for Y255C and I398T and retained 7% residual MPI activity. This patient had hypoglycemia, hyperinsulinemia, hepatomegaly, elevated transaminase levels, and reduced factor XI, antithrombin III, protein S, and protein C levels (27).

Mpi is an essential, nonredundant gene in mice. Surprisingly, both hypomorphic lines with very low residual MPI activity and those with altered mannose metabolism grew normally and failed to mimic any of the broad array of symptoms of patients with MPI-CDG. The activity was still sufficient for normal function in this strain. Limited outcrossing into a mixed 129/SV background also yielded no obvious pathological phenotype (data not shown).

We observed modest embryonic lethality in KI/KI mice that was presumably due to insufficient glycosylation. By analogy with mannose treatment of young patients with MPI-CDG, we assumed that mannose provided prenatally would correct the slight embryonic lethality. The results were opposite to our expectations. Mannose supplementation caused a dose-dependent lethality during gestation in KI/KI mice. This was likely due to high local mannose or Man-6-P concentration that alters glucose metabolism at a crucial time during development. The results of earlier studies showed that mannose provided at 5 mM slowed rat embryo development in culture and showed impaired neural tube morphogenesis (28). The teratogenic effect on rat

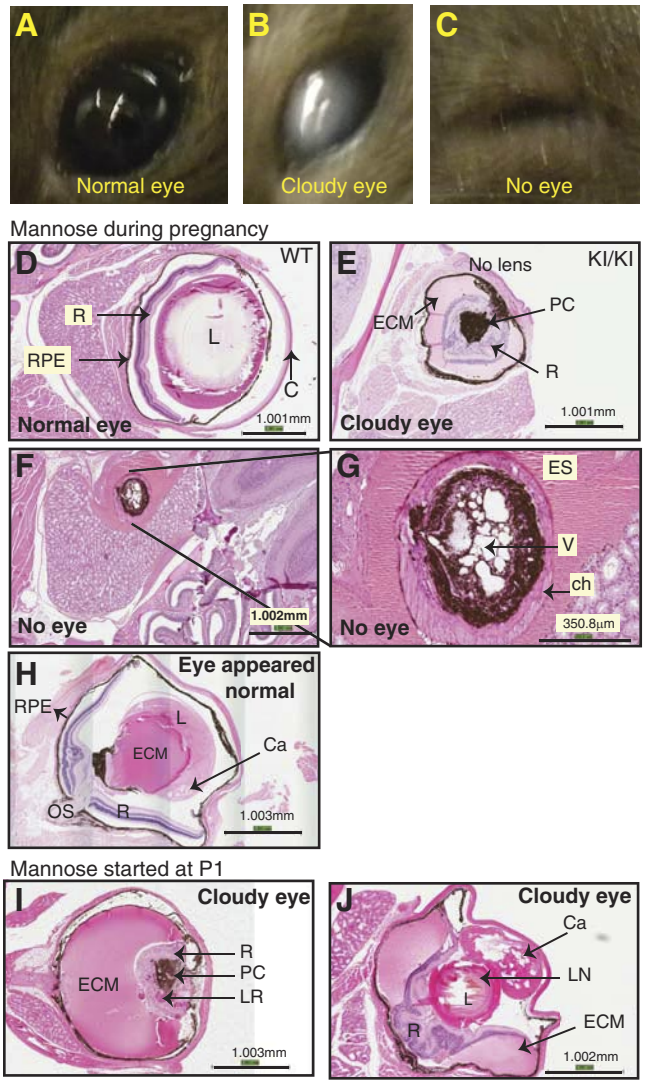

Figure 8. Appearence and histological images of adult mouse eyes. *A*) Normal eye. *B*) Cloudy eye. *C*) No eye phenotype. *D-J*) H&E stains of fixed eyes. *D*) Normal WT eye. *E–H*) Representative KI/KI eyes of mice that were maintained on mannose after being born to mannose-fed dams during conception and gestation. *E*) Eye with cloudiness evident at age 3 wk has no lens, distorted retina and a cluster of pigmented cells. *F*) Absence of an eye since birth shows as a small eye socket filled with vacuoles. *G*) Magnified view of panel *F*. *H*) Eye that appeared normal on physical examination showed deteriorating lens when sectioned and stained with H&E at 8 mo. *I, J*) Mannose supplementation was started at P1. *I*) Eye that showed cloudiness at age 3 wk has disintegrating lens and retina and infiltration of pigmented cells. *J*) Eye that turned cloudy at age 3 mo shows disintegrating lens. L, lens; R, retina; C, cornea; RPE, retinal pigmented epithelium; PC, pigmented cells; ES, eye socket; V, vacuole; Ch, choroid; ECM, extracellular matrix; OS, optic stalk; LR, lens remanants; LN, lens nucleus; Ca, cataract.

embryos was attributed to the impairment of glycolysis, and the effects could be reversed by glucose. Mannose was also found to be toxic to honeybees because of Man-6-P accumulation (29). Alternatively, Man-6-P may inhibit processes mediated by Man-6-P receptors, as expression of the two receptors is spatially and temporally regulated during mouse embryogenesis (30). One such example is proliferin, a placental growth and primary angiogenic factor expressed during midgestation (E8–E12; ref. 31), which binds to Man-6-P receptor on fetal and maternal tissue. This binding is abolished by mannose, but Man-6-P is 1000 times more effective (half maximal effect at 10 μM), suggesting a very specific effect of Man-6-P on the proliferin binding to one of the Man-6-P receptors (32).

In survivors, prenatal mannose affected only eye development in KI/KI animals. This is most likely due to higher mannose levels and lower MPI activity in the eyes than in all other major organs. Approximately 45% of animals developed ocular defects with varying degrees of severity, which suggests incomplete or reduced penetrance of the genetic mutation.

Histological analysis of eyes during embryonic development indicates failure to form a normal lens pit. This deformity initiates a cascade resulting in the absence of a lens, which is crucial for continued eye morphogenesis (33–35). Eyes lacking a lens grow slower, fail to accumulate vitreous substance, and are smaller (36, 37). Also, eyes devoid of a lens have a disorganized corneal endothelium and anterior segment (38). These findings suggest that extensive crosstalk occurs among the various cell types during eye development, with the lens being a major player. We do not know at which stage the initiation event leading to collapse of eye structure occurs; however, we could see inhibition of lens vesicle formation as early as E10.

Galactosemic cataracts are generally caused by galactose and galactitol accumulation due to lower galactose metabolic enzymes (39, 40). Hyperglycemia also causes cataracts to develop in those with diabetes (41). Aldol reductase, an enzyme with low specificity, causes polyol accumulation and is implicated in galactosemic and diabetic cataracts (42). Therefore, we expected an accumulation of mannitol in KI/KI eyes with mannose supplementation. However, mannitol did not accumulate despite elevated mannose levels in the affected/cloudy KI/KI eyes. The adverse effects are at least partially explained by the accumulation of mannose and Man-6-P in the affected KI/KI eyes. We also observed increased Man-6-P in KI/KI embryos but were unable to measure it specifically in embryonic eyes. Our data clearly show adverse effects on lens and amacrine cells in the retina. Other cell types could also be affected *via* several different mechanisms. For example, phagocytosis of photoreceptor outer segments by retinal pigmented epithelium is mediated by mannose receptors on the apical side and is inhibited specifically by mannose and mannans (43, 44). Also, transforming growth factor-β (TGF-β), which is critical for eye development (45) and is expressed in lens fibers around E14.5 through E17.5 (46), could be affected. TGF-β precursor activation is specifically inhibited by Man-6-P before binding to its receptor but not by Man-1-P (47).

KI/KI mice were continuously exposed to mannose during conception and gestation and after birth. Therefore, we do not know the time frame during

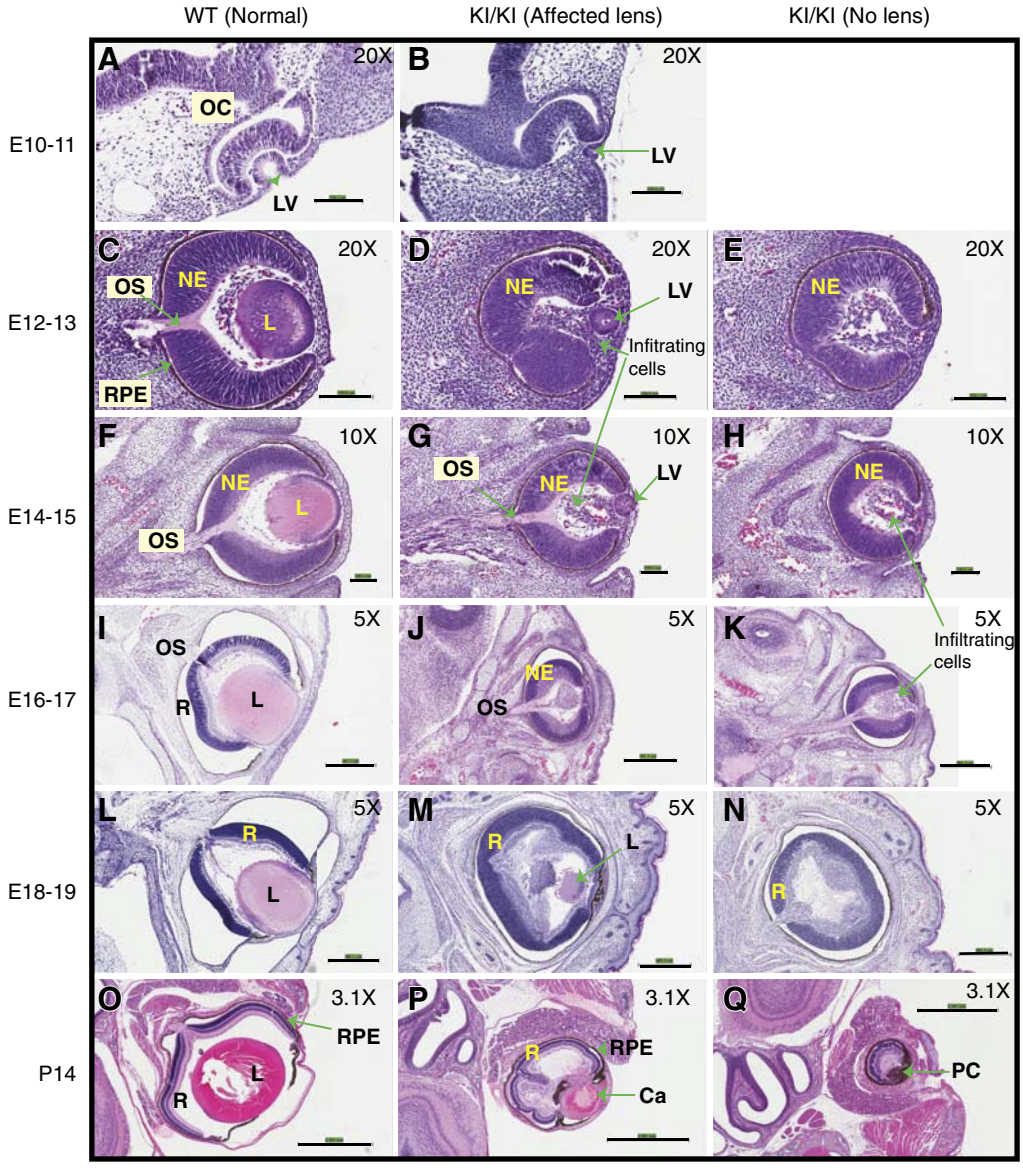

Figure 9. Eyes at various developmental stages. Timed matings were set up, and dams were provided 2% mannose throughout gestation. At indicated days, embryos were harvested and fixed. Paraffin sections were stained with H&E. Panels depict the histology of the eyes at E10–E11 (*A*, *B*), E12–E13 (*C–E*), E14–E15 (*F–H*), E16–E17 (*I–K*), E18–E19 (*L–N*), and P14 (*O–Q*). *A*, *C*, *F*, *I*, *L*, *O*) WT normal eyes. *B*, *D*, *G*, *J*, *M*, *P*) KI/KI eyes with affected lens. *E*, *H*, *K*, *N*, *Q*) KI/KI eyes with no lens. OC, optic cup; LV, lens vesicle; NE, neuroepithelium; L, lens; OS, optic stalk; RPE, retinal pigmented epithelium; PC, pigmented cells; Ca, cataract. Magnification is the same for WT and KI/KI at each development stage, although it varies among stages, high (×10–20) for early embryonic stages and low (×3.1–5) for later embryonic stages and postbirth. Scale bars = 100 μm (*A–H*); 400 μm (*I–N*); 1 mm (*O–Q*).

early development when embryos are most susceptible to mannose. The first indications of mannose-induced embryo demise and impaired lens development occur around E10.5. This coincides with the death of both previously reported *Mpi*-null and hypomorphic $Pmm2^{R137H/F118L}$ embryos (3, 19). All have placental abnormalities. Man-6-P accumulation in *Mpi*-null (3) and mannose-exposed KI/KI embryos presumably contributes to their death, while insufficient glycosylation is lethal for $Pmm2^{R137H/F118L}$ embryos (19). Providing ~1% mannose in the drinking water of $Pmm2^{R137H/F118L}$-bearing dams rescues insufficient glycosylation and ensures pup survival beyond weaning. Notably, the same amount of mannose that rescues this strain is teratogenic or lethal in the KI/KI genotype. In both cases, the dams show only a nominal (1.4- to 1.7-fold) increase in their blood mannose concentration, suggesting that moderate changes in metabolite concentrations lead to drastic outcomes. These results underscore the importance of regulation of mannose concentration during embryonic development. Man-6-P is a common substrate for both MPI and PMM2. The ratio of PMM2:MPI activity determines the

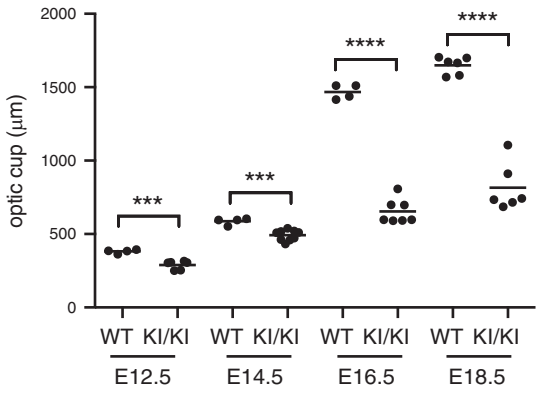

Figure 10. Optic cup measurement. Length of the cross-section of the optic cup of the fixed H&E-stained eyes was measured by using Aperio software. ***$P < 0.0005$; ****$P < 0.0001$.

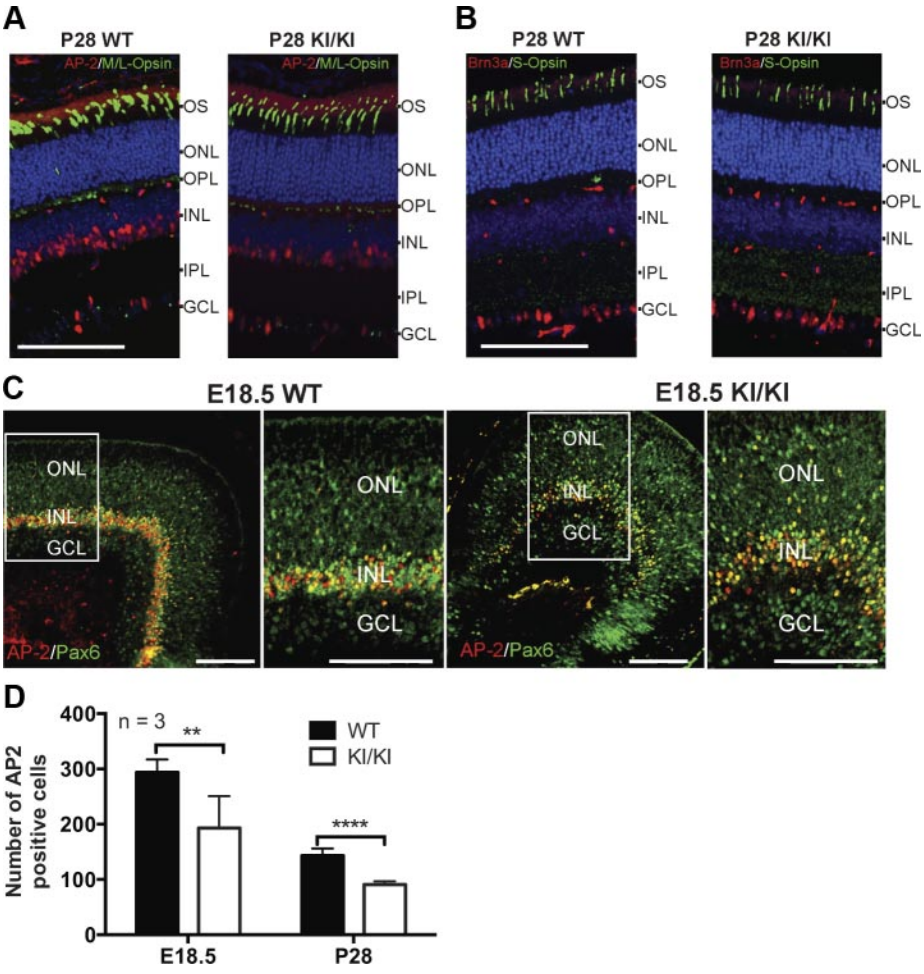

Figure 11. Immunofluorescence of WT and KI/KI eye sections. *A*) staining with AP-2, an amacrine-specific cell marker (in red), in the inner nuclear layer and M/L opsin (for red and green opsins), a cone photoreceptor cell marker (in green), for outer segments on P28 WT and KI/KI eyes. Scale bar = 100 μm. *B*) Staining with Brn3a, a ganglion cell marker (in red), in the ganglion cell layer and S opsin, a blue opsin cone photoreceptor cell marker (in green), in the outer segments of P28 WT and KI/KI sections. Scale bar = 100 μm. *C*) Staining with Pax6, a ganglion and amacrine cell marker (in green), and AP-2 (in red) on E18.5 WT and KI/KI eyes. Right panels show enlarged views of the boxed areas in left panels. GCL, ganglion cell layer; IPL, inner plexiform layer; INL, inner nuclear layer; OPL, outer plexiform layer; ONL, outer nuclear layer; OS, outer segments. *D*) ImageJ software was used to count the number of AP2-immunopositive cells from the posterior region of 2 different ×40 confocal images from 3 different eyes and calculate means ± SD. $^{**}P < 0.005$, $^{****}P < 0.0001$.

metabolic flux and steady state of Man-6-P (5). Imbalance of this ratio in *Mpi* hypomorphic embryos makes them incapable of coping with the increased mannose influx. Man-6-P was not reported in the *Pmm2*$^{R137H/F118L}$ embryos (19).

It is uncertain whether the results of mannose supplementation using *Mpi* in this study or *Pmm2* hypomorphic mice (19) can be extrapolated to humans. Based on the published results that mannose supplementation rescues *mpi*-morpholino-mediated knock-

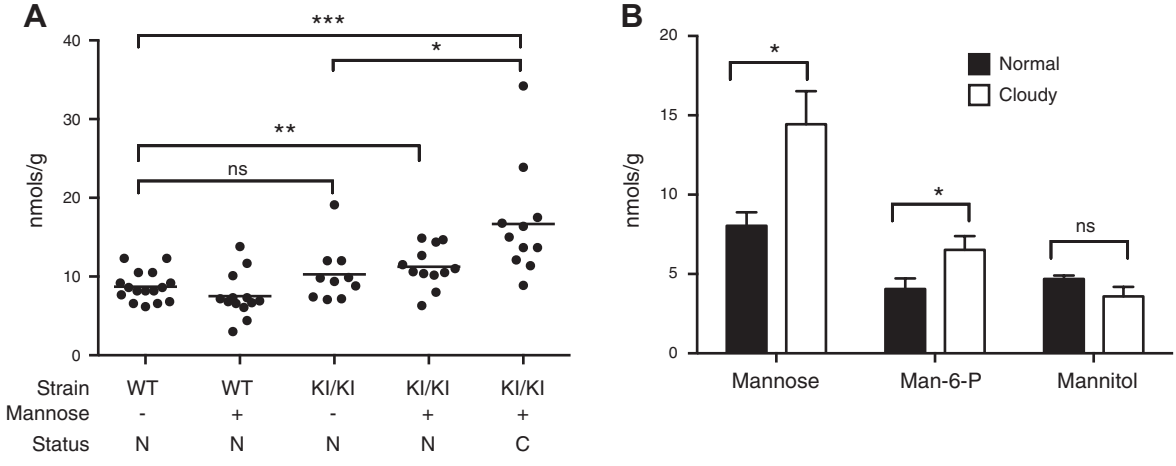

Figure 12. Measurement of metabolites in the eyes. *A*) A coupled fluorescent assay was used to measure the concentration of Man-6-P in the eyes of WT and KI/KI mice supplemented with or without mannose. Status of the eye is represented by *n* = not affected. C = cloudy. *B*) Mannose, Man-6-P and mannitol concentrations were estimated by GC-MS of the normal and affected eyes of mannose-fed KI/KI mice. Bars represent means ± SEM of 5 mice. ns, not significant. $^{*}P < 0.05$, $^{**}P < 0.005$, $^{***}P < 0.001$.

down in zebrafish embryos (MPI-CDG model) and reverses lethality of *Pmm2* hypomorphic mouse embryos (PMM2-CDG model) when started before conception and continued through gestation till birth, physicians might encourage mothers of children with MPI-CDG to take mannose during a subsequent pregnancy to prevent symptoms that might develop during gestation. However, on the basis of our limited results, we strongly advise against this action. Similarly, we regard the recommendation made by an earlier publication (19) that mothers at risk of having babies with PMM2-CDG consume mannose during pregnancy to overcome the symptoms of PMM2-CDG *in utero* as being highly premature. A narrow window of mannose metabolic flux may determine normal *vs.* pathological state during embryogenesis, as demonstrated in Fig. 7*A*, where there is a significant increase in Man-6-P levels even in WT mice supplemented with 2% mannose. A similar study to demonstrate toxicity in humans is not feasible.

Mannose is also widely sold as a urinary tract health supplement. It is known to competitively inhibit binding of infectious *Escherichia coli* to urinary tract of mice (48), and recently, the first human clinical trial showed mannose as an effective prophylactic agent with minimal side effects (49). The widespread use of mannose as a risk-free, Internet-available, "natural glyconutrient" remedy for urinary tract infections underscores the need for caution, especially during pregnancy, since the prevalence of MPI-CDG is unknown. FJ

This work was supported by grants from the U.S. National Institutes of Health (R01-DK55615), the Children's Heart Fund, and the Rocket Fund (to H.H.F.). The authors thank Dr. Peter Westenskow [The Scripps Research Institute (TSRI), La Jolla, CA, USA] for sharing some of the antibodies. The authors also thank Dr. Amanda Roberts (TSRI mouse behavioral assessment core) for providing access to the optic drum. The authors greatly appreciate Guillermina Garcia and Robbin Newlin [Sanford-Burnham Medical Research Institute (SBMRI) histology core facility] for exceptional technical support with histology. The authors thank the SBMRI animal facility staff for setting up the mouse breeding and taking care of the animals and Buddy Charbono for technical support. The authors also acknowledge technical support provided by Jamie Smolin in their laboratory.

REFERENCES

1. Niehues, R., Hasilik, M., Alton, G., Körner, C., Schiebe-Sukumar, M., Koch, H. G., Zimmer, K. P., Wu, R., Harms, E., Reiter, K., von Figura, K., Freeze, H. H., Harms, H. K., and Marquardt, T. (1998) Carbohydrate-deficient glycoprotein syndrome type Ib. Phosphomannose isomerase deficiency and mannose therapy. *J. Clin. Invest.* **101,** 1414–1420
2. De Lonlay, P., and Seta, N. The clinical spectrum of phosphomannose isomerase deficiency, with an evaluation of mannose treatment for CDG-Ib. (2009) *Biochim. Biophys. Acta* **1792,** 841–843
3. DeRossi, C., Bode, L., Eklund, E. A., Zhang, F., Davis, J. A., Westphal, V., Wang, L., Borowsky, A.D., and Freeze, H. H. (2006) Ablation of mouse phosphomannose isomerase (Mpi) causes mannose 6-phosphate accumulation, toxicity, and embryonic lethality. *J. Biol. Chem.* **281,** 5916–5927
4. Davis, J. A., Wu, X. H., Wang, L., DeRossi, C., Westphal, V., Wu, R., Alton, G., Srikrishna, G., and Freeze, H. H. (2002) Molecular cloning, gene organization, and expression of mouse Mpi encoding phosphomannose isomerase. *Glycobiology* **12,** 435–442
5. Sharma, V., and Freeze, H. H. (2011) Mannose efflux from the cells: a potential source of mannose in blood. *J. Biol. Chem.* **286,** 10193–10200
6. Sharma, V., Ichikawa, M., He, P., Scott, D. A., Bravo, Y., Dahl, R., Ng, B. G., Cosford, N. D., and Freeze, H. H. (2011) Phosphomannose isomerase inhibitors improve N-glycosylation in selected phosphomannomutase-deficient fibroblasts. *J. Biol. Chem.* **286,** 39431–39438
7. Gracy, R. W., and Noltmann, E. A. (1968) Studies on phosphomannose isomerase. I. Isolation, homogeneity measurements, and determination of some physical properties. *J. Biol. Chem.* **243,** 3161–3168
8. Crossley, J. R., and Elliott, R. B. (1977) Simple method for diagnosing protein-losing enteropathies. *Br. Med. J.* **1,** 428–429
9. Price, N. P. (2004) Acylic sugar derivatives for GC/MS analysis of 13C-enrichment during carbohydrate metabolism. *Anal. Chem.* **76,** 6566–6574
10. Donthi, R. V., and Epstein, P. N. (2007) Altering and analyzing glucose metabolism in perfused hearts of transgenic mice. *Methods Mol. Med.* **139,** 151–161
11. Zhu, A., Romero, R., and Petty, H. R. (2009) An enzymatic fluorimetric assay for glucose-6-phosphate: application in an in vitro Warburg-like effect. *Anal. Biochem.* **388,** 97–101
12. Cline, A., Gao, N., Flanagan-Steet, H., Sharma, V., Rosa, S., Sonon, R., Azadi, P., Sadler, K. C., Freeze, H. H., Lehrman, M. A., and Steet, R. (2012) A zebrafish model of PMM2-CDG reveals altered neurogenesis and a substrate-accumulation mechanism for N-linked glycosylation deficiency. *Mol. Biol. Cell* **23,** 4175–4187
13. Chu, J., Mir, A., Gao, N., Rosa, S., Monson, C., Sharma, V., Steet, R., Freeze, H. H., Lehrman, M. A., and Sadler, K. C. (2012) A zebrafish model of congenital disorders of glycosylation with phosphomannose isomerase deficiency reveals an early opportunity for corrective mannose supplementation. *Dis. Model. Mech.* **6,** 95–105
14. Halket, J. M., and Zaikin, V. G. (2003) Derivatization in mass spectrometry–1. Silylation. *Eur. J. Mass. Spectrom. (Chichester, Eng.)* **9,** 1–21
15. Michelakakis, H., Moraitou, M., Mavridou, I., and Dimitriou, E. (2009) Plasma lysosomal enzyme activities in congenital disorders of glycosylation, galactosemia and fructosemia. *Clin. Chim. Acta* **401,** 81–83
16. Marklová, E., and Albahri, Z. (2007) Screening and diagnosis of congenital disorders of glycosylation. *Clin. Chim. Acta* **385,** 6–20
17. Bode, L., Salvestrini, C., Park, P. W., Li, J. P., Esko, J. D., Yamaguchi, Y., Murch, S., and Freeze, H. H. (2008) Heparan sulfate and syndecan-1 are essential in maintaining murine and human intestinal epithelial barrier function. *J. Clin. Invest.* **118,** 229–238
18. Davis, J. A., and Freeze, H. H. (2001) Studies of mannose metabolism and effects of long-term mannose ingestion in the mouse. *Biochim. Biophys. Acta* **1528,** 116–126
19. Schneider, A., Thiel, C., Rindermann, J., DeRossi, C., Popovici, D., Hoffmann, G. F., Grone, H. J., and Korner, C. (2011) Successful prenatal mannose treatment for congenital disorder of glycosylation-Ia in mice. *Nat. Med.* **18,** 7–73
20. Thiel, C., Lübke, T., Matthijs, G., von Figura, K., and Körner, C. (2006) Targeted disruption of the mouse phosphomannomutase 2 gene causes early embryonic lethality. *Mol. Cell. Biol.* **26,** 5615–5620
21. Marek, K. W., Vijay, I. K., and Marth, J. D. (1999) A recessive deletion in the GlcNAc-1-phosphotransferase gene results in peri-implantation embryonic lethality. *Glycobiology* **9,** 1263–1271
22. Cantagrel, V., Lefeber, D. J., Ng, B. G., Guan, Z., Silhavy, J. L., Bielas, S. L., Lehle, L., Hombauer, H., Adamowicz, M., Swiezewska, E., De Brouwer, A. P., Blümel, P., Sykut-Cegielska, J., Houliston, S., Swistun, D., Ali, B. R., Dobyns, W. B., Babovic-Vuksanovic, D., van Bokhoven, H., Wevers, R. A., Raetz, C. R., Freeze, H. H., Morava, E., Al-Gazali, L., and Gleeson, J. G. (2010) SRD5A3 is required for converting polyprenol to dolichol and is mutated in a congenital glycosylation disorder. *Cell* **142,** 203–217

23. Wang, Y., Tan, J., Sutton-Smith, M., Ditto, D., Panico, M., Campbell, R. M., Varki, N. M., Long, J. M., Jaeken, J., Levinson, S. R., Wynshaw-Boris, A., Morris, H. R., Le, D., Dell, A., Schachter, H., and Marth, J. D. (2001) Modeling human congenital disorder of glycosylation type IIa in the mouse: conservation of asparagine-linked glycan-dependent functions in mammalian physiology and insights into disease pathogenesis. *Glycobiology* **11,** 1051–1070
24. Hellbusch, C. C., Sperandio, M., Frommhold, D., Yakubenia, S., Wild, M. K., Popovici, D., Vestweber, D., Gröne, H. J., von Figura, K., Lübke, T., and Körner, C. (2007) Golgi GDP-fucose transporter-deficient mice mimic congenital disorder of glycosylation IIc/leukocyte adhesion deficiency II. *J. Biol. Chem.* **282,** 10762–10772
25. Lu, Q., Hasty, P., and Shur, B. D. (1997) Targeted mutation in beta1,4-galactosyltransferase leads to pituitary insufficiency and neonatal lethality. *Dev. Biol.* **181,** 257–267
26. Asano, M., Furukawa, K., Kido, M., Matsumoto, S., Umesaki, Y., Kochibe, N., and Iwakura, Y. (1997) Growth retardation and early death of beta-1,4-galactosyltransferase knockout mice with augmented proliferation and abnormal differentiation of epithelial cells. *EMBO J.* **16,** 1850–1857
27. De Lonlay, P., Cuer, M., Vuillaumier-Barrot, S., Beaune, G., Castelnau, P., Kretz, M., Durand, G., Saudubray, J. M., and Seta, N. (1999) Hyperinsulinemic hypoglycemia as a presenting sign in phosphomannose isomerase deficiency: a new manifestation of carbohydrate-deficient glycoprotein syndrome treatable with mannose. *J. Pediatr.* **135,** 379–383
28. Buchanan, T., Freinkel, N., Lewis, N. J., Metzger, B. E., and Akazawa, S. (1985) Fuel-mediated teratogenesis. Use of D-mannose to modify organogenesis in the rat embryo in vivo. *J. Clin. Invest.* **75,** 1927–1934
29. Sols, A., Cadenas, E., and Alvarado, F. (1960) Enzymatic basis of mannose toxicity in honey bees. *Science* **131,** 297–298
30. Matzner, U., von Figura, K., and Pohlmann, R. (1992) Expression of the two mannose 6-phosphate receptors is spatially and temporally different during mouse embryogenesis. *Development* **114,** 965–972
31. Jackson, D., Volpert, O. V., Bouck, N., and Linzer, D. I. (1994) Stimulation and inhibition of angiogenesis by placental proliferin and proliferin-related protein. *Science* **266,** 1581–1584
32. Lee, S. J., and Nathans, D. (1988) Proliferin secreted by cultured cells binds to mannose 6-phosphate receptors. *J. Biol. Chem.* **263,** 3521–3527
33. Genis-Galvez, J. M. (1966) Role of the lens in the morphogenesis of the iris and cornea. *Nature* **210,** 209–210
34. Breitman, M. L., Bryce, D. M., Giddens, E., Clapoff, S., Goring, D., Tsui, L. C., Klintworth, G. K., and Bernstein, A. (1989) Analysis of lens cell fate and eye morphogenesis in transgenic mice ablated for cells of the lens lineage. *Development* **106,** 457–463
35. Yamamoto, Y., and Jeffery, W. R. (2000) Central role for the lens in cave fish eye. *Degeneration* **289,** 631–633
36. Coulombre, A. J., and Coulombre, J. L. (1964) Lens development. I. Role of the lens in eye growth. *J. Exp. Zool.* **156,** 39–47
37. Coulombre, A. J., and Herrmann, H. (1965) Lens development. 3. Relationship between the growth of the lens and the growth of the outer eye coat. *Exp. Eye Res.* **4,** 302–311
38. Beebe, D. C., and Coats, J. M. (2000) The lens organizes the anterior segment: specification of neural crest cell differentiation in the avian eye. *Dev. Biol.* **220,** 424–431
39. Kinoshita, J. H. (1965) Cataracts in galactosemia. The Jonas S. Friedenwald Memorial Lecture. *Invest. Ophthalmol.* **4,** 786–799
40. Gitzelmann, R., Curtius, H. C., and Schneller, I. (1967) Galactitol and galactose-1-phosphate in the lens of a galactosemic infant. *Exp. Eye Res.* **6,** 1–3
41. Varma, S. D., Schocket, S. S., and Richards, R. D. (1979) Implications of aldose reductase in cataracts in human diabetes. *Invest. Ophthalmol. Vis. Sci.* **18,** 237–241
42. Dvornik, E., Simard-Duquesne, N., Krami, M., Sestanj, K., Gabbay, K. H., Kinoshita, J. H., Varma, S. D., and Merola, L. O. (1973) Polyol accumulation in galactosemic and diabetic rats: control by an aldose reductase inhibitor. *Science* **182,** 1146–1148
43. Boyle, D., Tien, L. F., Cooper, N. G., Shepherd, V., and McLaughlin, B. J. (1991) A mannose receptor is involved in retinal phagocytosis. *Invest. Ophthalmol. Vis. Sci.* **32,** 1464–1470
44. Wilt, S. D., Greaton, C. J., Lutz, D. A., and McLaughlin, B. J. (1999) Mannose receptor is expressed in normal and dystrophic retinal pigment epithelium. *Exp. Eye Res.* **69,** 405–411
45. Saika, S. (2006) TGFbeta pathobiology in the eye. *Lab. Invest.* **86,** 106–115
46. Pelton, R. W., Saxena, B., Jones, M., Moses, H. L., and Gold, L. I. (1991) Immuno-histochemical localization of TGF beta 1, TGF beta 2, and TGF beta 3 in the mouse embryo: expression patterns suggest multiple roles during embryonic development. *J. Cell Biol.* **115,** 1091–1105
47. Dennis, P. A., and Rifkin, D. B. (1991) Cellular activation of latent transforming growth factor beta requires binding to the cation-independent mannose 6-phosphate/insulin-like growth factor type II receptor. *Proc. Natl. Acad. Sci. U. S. A.* **88,** 580–584
48. Aronson, M., Medalia, O., Schori, L., Mirelman, D., Sharon, N., and Ofek, I. (1979) Prevention of colonization of the urinary tract of mice with *Escherichia coli* by blocking of bacterial adherence with methyl alpha-D-mannopyranoside. *J. Infect. Dis.* **139,** 329–332
49. Kranjcec, B., Papes, D., and Altarac, S. (2013) D-mannose powder for prophylaxis of recurrent urinary tract infections in women: a randomized clinical trial. [E-pub ahead of print]. *World J. Urol.* doi:10.1007/s00345-013-1091-6

Received for publication October 28, 2013.
Accepted for publication January 2, 2014.